



## Sulfur tolerant Co–Mo–K catalysts supported on carbon materials for sour gas shift process – Effect of support modification



Katarzyna Antoniak-Jurak <sup>a,\*</sup>, Paweł Kowalik <sup>a</sup>, Marcin Konkol <sup>a</sup>, Wiesław Próchniak <sup>a</sup>, Robert Bicki <sup>a</sup>, Wioletta Raróg-Pilecka <sup>b</sup>, Piotr Kuśtrowski <sup>c</sup>, Janusz Ryczkowski <sup>d</sup>

<sup>a</sup> New Chemical Syntheses Institute, Catalyst Research Department, Al. Tysiąclecia Państwa Polskiego 13A, 24-110 Puławy, Poland

<sup>b</sup> Warsaw University of Technology, Faculty of Chemistry, Noakowskiego 3, 00-662 Warsaw, Poland

<sup>c</sup> Jagiellonian University, Faculty of Chemistry, Ingardena 3, 30-060 Kraków, Poland

<sup>d</sup> University of Maria Curie-Skłodowska, Faculty of Chemistry, Department of Chemical Technology, pl. M. Curie-Skłodowskiej 3, 20-031 Lublin, Poland

### ARTICLE INFO

#### Article history:

Received 30 October 2015

Received in revised form 2 January 2016

Accepted 11 January 2016

Available online xxxx

#### Keywords:

Sour gas shift

Carbon supported Co–Mo–K catalysts

Carbon black composites

Mesoporous carbon support

### ABSTRACT

The effect of steam gasification on the surface composition, surface area, pore size distribution as well as on the morphology of the carbon supports has been investigated. Materials have been characterized by nitrogen physisorption, mercury porosimetry, X-ray diffraction (XRD), X-ray photoelectron spectroscopy (XPS) and transmission electron microscopy (TEM). Model samples of the Co–Mo–K catalysts with the same composition have been prepared on carbon supports differing in the temperature of steam gasification process. Catalytic activity measurements have been carried out in a gradientless reactor in a kinetic regime at low partial pressures of reagents. A relationship between textural parameters of the supports and the catalysts activity has been estimated. The highest activity in the SGS process has been determined for the Co–Mo–K/SRO/40.49 supported catalyst.

© 2016 Elsevier B.V. All rights reserved.

### 1. Introduction

The usefulness of carbon supports in catalysis results from their specific physicochemical properties, especially from a possibility of obtaining large specific surface areas up to  $>1000 \text{ m}^2/\text{g}$  (or even  $>3000 \text{ m}^2/\text{g}$ ) [1], from their high stability within high temperature ranges, easy recovery of an active phase from spent catalysts through burning of the carbon support, from a relatively easy modifiability as well as from much weaker support–active phase interactions as a result of carbon surface specificities [2].

There have been several attempts to utilize the carbon-supported Co–Mo and Ni–Mo catalyst in hydrodesulphurization processes [3] and higher alcohols synthesis [4,5,6]. Moreover, the application of carbon-based catalysts in hydrodechlorination processes of chlorofluorocarbon compounds (CFC) seems to be also of interest [7]. While reports in the literature concerning the carbon-supported Co–Mo catalysts used in the HDS reactions are extensive [3,8] analogous examples on the application of these catalytic systems in the SGS process are relatively sparse [9,10]. To the best of our knowledge only two reports on carbon-supported catalysts in the SGS reaction are dedicated to the Co–Mo–K system.

Alkali-promoted Co–Mo catalyst is suitable for processing the products of coal or biomass gasification [11]. In spite of numerous advantages of carbon-based catalysts, their industrial application is strongly limited. Practically, only Co–Mo catalysts supported on  $\text{Al}_2\text{O}_3$  or  $\text{MgO-Al}_2\text{O}_3$  [12–20] have found the application in the SGS process, although there is a number of literature contributions on the utilization of other supports [21–24]. Recently, there has been an increasing interest in cesium-doped Co–Mo catalysts [25], which are very active even at low  $\text{H}_2\text{S}$  content in the process gas [26].

The limited applicability of carbon supports in industrial catalysis results from unquestionable disadvantages of raw carbon materials including, in particular, a high content of mineral impurities, unfavorable pore structure characterized by a relatively high micropore presence that generates diffusion resistances, facilitates the mechanical blocking and limits the active surface availability [2,27]. Furthermore, carbon materials exhibit relatively low mechanical strength and due to the potential methanation reaction they should not be used in the presence of hydrogen at temperatures exceeding 700 K [28]. Thus, a wider application of carbon materials as catalyst supports is strongly related to the improvement of active carbons properties and these materials are a subject of various modifications.

Our present contribution is strictly related to the subject area of the previous work [10]. Co–Mo–K catalysts prepared on modified active carbon had substantially higher activity than that supported on flash calcined alumina. Such effect was found even for Co–Mo K/NRO/1900

\* Corresponding author.

E-mail address: [katarzyna.antoniak@ins.pulawy.pl](mailto:katarzyna.antoniak@ins.pulawy.pl) (K. Antoniak-Jurak).

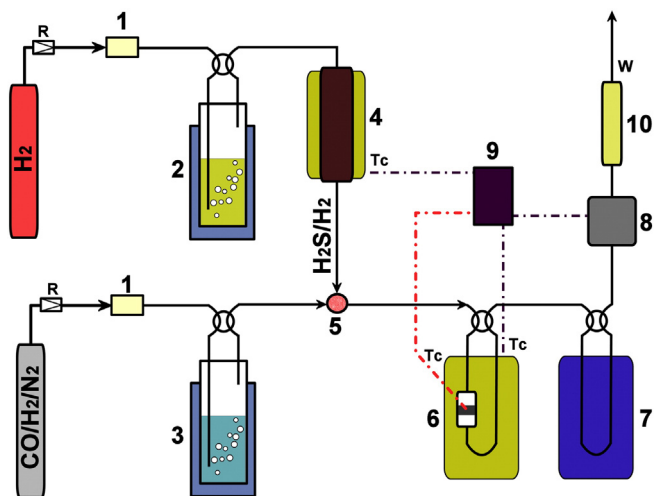


Fig. 1. Flow diagram of the reaction system for determination of the catalysts activity: 1 – gas steam regulators, 2 – H<sub>2</sub>S generator, 3 – steam generator, 4 – reactor with Ni-Mo/Al<sub>2</sub>O<sub>3</sub>, 5 – mixer, 6 – gradientless reactor, 7 – dry ice cold trap, 8 – gas flow analyzer, 9 – PC, 10 – flowmeter.

catalyst, i.e. system which was supported on carbon with the lowest specific surface area and porosity. The highest activity in the SGS reaction was obtained for sulfided catalysts supported on NRO/1900/33.3 and can be related with specific surface area of carbon support.

As reported in our previous work [10] the removal of mineral impurities leading to the improvement of porous structure (more pores with a diameter > 2 nm) can be achieved by thermal treatment of raw carbons at high temperature (1900 °C) in helium atmosphere and subsequent partial gasification with steam. However, this processing may cause deterioration of the mechanical strength. The improvement of texture properties with maintaining high mechanical strength of carbon supports can be realized by the application of carbon black composites for the preparation of carbon materials [29,30].

One of such material is *Sibunit*, prepared by pyrolysis of C1–C3 hydrocarbons at 850–950 °C. A detailed description of the *Sibunit* preparation process has been reported in work [31]. *Sibunit* is used as the support of catalysts for various processes [32]. Undoubtedly, *Sibunit* has a beneficial texture (in the range that could be important for the catalytic properties of support materials), high purity and higher thermal stability than conventional active carbons. It seems to be especially promising support of highly dispersed Co–Mo–S phase of type II, which is characterized by no Mo–O–S species [33,34]. Thanks to this feature a higher degree of reduction and sulphidation can be achieved that in consequence results in a higher catalytic activity compared to systems supported on alumina [35]. From the technological viewpoint of WGS process it is also preferred to decrease the process temperature (beneficial shift of the equilibrium), which requires the development of low-temperature catalysts.

In the present study a detailed characteristics of carbon supports was carried out in order to get a support with desired and defined properties for the preparation of highly active catalysts for the low temperature SGS process. The catalytic activity of several model carbon-supported Co–Mo–K samples with the same content of Mo, Co and K was evaluated in the SGS process at the temperature range 200–350 °C and in the presence of H<sub>2</sub>S.

## 2. Experimental

### 2.1. Preparation

The commercial material *Sibunit* (denoted as SRO, in the form of balls of a diameter in the range 0.5–1.0 mm) was used as a starting material. Partial steam gasification of SRO was carried out in a tubular

furnace in the presence of H<sub>2</sub>O/Ar mixture generated by passing at 675, 800, 835 or 850 °C for 5 h the stream of argon at the total flow rate of 15 l/h through an evaporator filled with H<sub>2</sub>O to achieve the steam flow of 19 ml/h. The obtained materials were washed with distilled water in order to remove the dust fraction and then dried at 120 °C for 24 h in air. The prepared materials were denoted as SRO/3.8, SRO/13.95, SRO/32.42 and SRO/40.49.

All catalysts were prepared using the impregnation method, according to the procedure described in our previous contributions [10,24]. The nominal content composition of the precursors was 16 wt% MoO<sub>3</sub> and 4 wt% CoO, the promoter content expressed as a K/Mo molar ratio was 0.1. The prepared catalyst samples were marked with the following

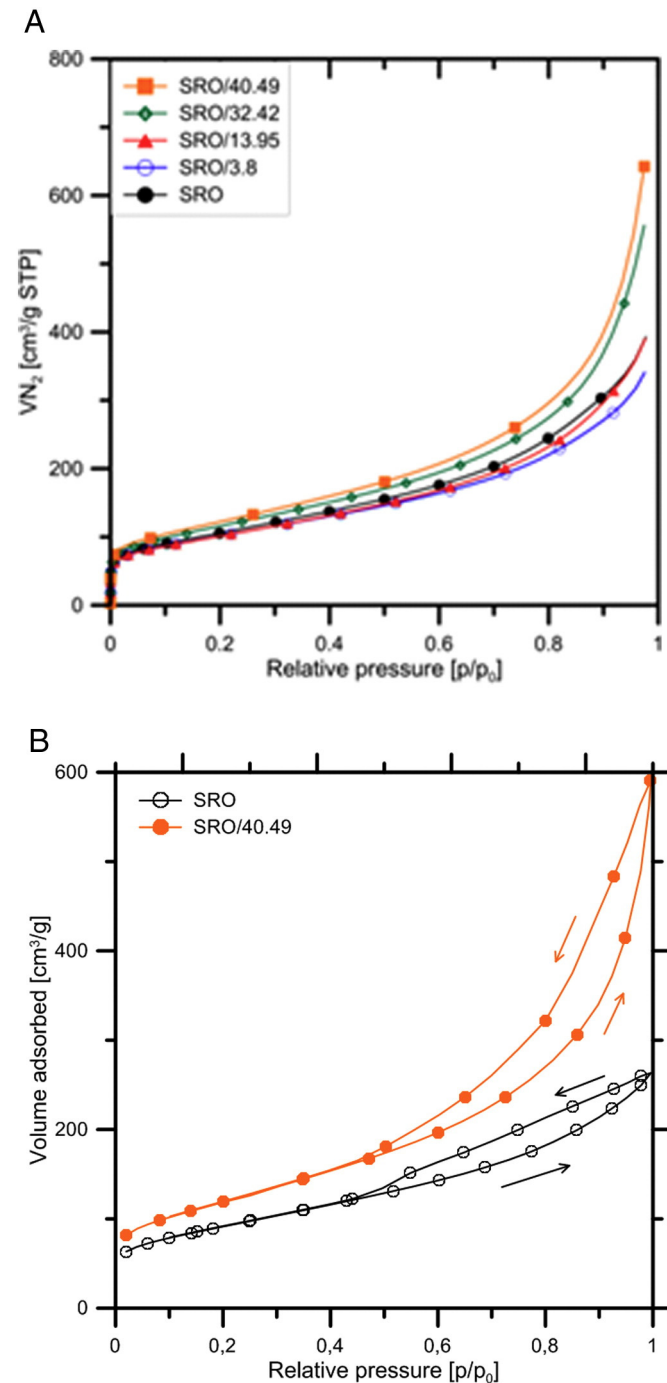


Fig. 2. Nitrogen adsorption-desorption isotherms of the initial carbon SRO and modified carbon materials.

**Table 1**  
Textural parameters of carbon materials determined by nitrogen physisorption analysis.

Sample	Surface area $m^2/g$			Pore volume $[cm^3/g]$			$D^e$ meso BJH [nm]
	SBET <sup>a</sup>	t-Plot <sup>b</sup> micropores	t-Plot <sup>b</sup> meso- and macropores	Total volume HK <sup>c</sup>	Micropores t-plot	Mesopores BJH <sup>d</sup>	
SRO	364	16	350	0.61	0.01	0.52	15.6
SRO/3.8	359	56	303	0.53	0.04	0.44	14.2
SRO/13.95	360	17	342	0.60	0.01	0.52	16.4
SRO/32.42	412	0	412	0.86	–	0.77	20.9
SRO/40.49	435	0	435	0.99	–	0.89	22.6

<sup>a</sup> Surface area calculated using Brunauer–Emmett–Teller (BET) method.

<sup>b</sup> Surface area micropores, mesopores and macropores.

<sup>c</sup> Total pore volume.

<sup>d</sup> Pore volume mesopores from Barret–Joyner–Halenda (BJH) analysis.

<sup>e</sup> Average pore diameters.

symbols: Co–Mo–K/SRO, Co–Mo–K/SRO/3.8, Co–Mo–K/SRO/13.95, Co–Mo–K/SRO/32.42 and Co–Mo–K/SRO/40.49.

## 2.2. Characterization

The  $N_2$  adsorption and desorption processes at  $-196^\circ C$  were studied on a Micromeritics ASAP 2020 instrument. The specific surface area,  $S_{BET}$ , was calculated according to the classical Brunauer–Emmett–Teller theory (BET). The t-plot method was used to determine the surface area and micropores volume. The average micropores size ( $D_{micro}$ ) was determined with the HK (Horvath–Kawazoe) method. The same model was applied for calculations of the total volume of micropores. The mesopores volume and average mesopores size ( $D_{meso}$ ) was determined using the BJH (Barret–Joyner–Halenda) method.

Mercury porosimetry studies were carried out up to 400 MPa using an AutoPore IV 9510 apparatus (Micromeritics Instrument Co.).

The X-ray photoelectron spectra (XPS) of the carbon materials were recorded on a Prevac photoelectron spectrometer equipped with a hemispherical VG SCIENTA R3000 analyzer. The spectra were collected using a monochromatized aluminum source  $AlK\alpha$  ( $E = 1486.6$  eV). The base pressure in the analytical chamber was  $5 \times 10^{-9}$  mbar. The binding energy values of measured regions were referenced to the Au 4f7/2 core level (84.0 eV). The surface composition was studied based on the areas and binding energies of C 1s, O 1s, and Fe 2p core levels. Fitting of the high resolution spectra was performed using the CasaXPS software.

The XRD measurements were performed on a PANalytical Empyrean system (Bragg–Brentano geometry) equipped with a PIXcel3D detector using  $Cu K\alpha$  radiation ( $\lambda = 1.542$  Å) and operating at 40 kV and 40 mA.

A high resolution electron transmission microscope Titan3 G2 60–300 (FEI Co.) was applied to analyze selected carbons. The observations were made at magnifications from 70kx to 1.2 Mx at beam energy of 300 keV (which corresponds to spacial resolution of about 80 pm).

## 2.3. Activity tests

SGS rate measurements were performed in a quartz gradientless reactor at the temperature range of 200–350 °C and pressure of 0.1 MPa. A

**Table 2**  
Textural parameters of carbon materials determined by mercury porosimetry.

Carbon sample	$S_{HC}^a$ [ $m^2/g$ ]	$V_{Hg}^b$ [ $cm^3/g$ ]	$V_{mHg}^c$ [ $cm^3/g$ ]	Porosity [%]	% Me <sup>d</sup>
SRO	177	0.56	0.46	47	86
SRO/3.8	205	0.64	0.54	52	86
SRO/13.95	202	0.66	0.56	53	87
SRO/32.42	264	1.13	0.86	64	79
SRO 40.49	256	1.23	0.88	65	75

<sup>a</sup> Pore surface area determined by porosimetry.

<sup>b</sup> Pore volume available for mercury intrusion.

<sup>c</sup> Mesopores volume from the range 3–80.

<sup>d</sup> Fraction of mesopores volume in the total pore volume.

catalyst sample (150 mg) grounded to the fraction of 0.1–0.16 mm was placed into the reactor and loaded with a process gas containing  $H_2S$ . Detailed description of the catalyst activation and measurement procedures was reported in [24]. As a measure of the catalytic activity, a reaction rate related to a catalyst weight unit,  $r[Ndm^3/g_{cat} \cdot h]$ , at degree of conversion  $X = 20\%$  was used. A scheme of laboratory equipment used for studying of catalytic activity is shown in Fig. 1.

## 3. Results and discussion

### 3.1. Textural properties of the carbon supports

The nitrogen adsorption–desorption isotherms at  $-196^\circ C$  are shown in Fig. 2A and B.

The shape of isotherms for the series of carbon supports is similar to type IV (according to IUPAC classification) [36]. The hysteresis loop for the carbon support SRO/40.49 is typical for the H3 hysteresis type but for the carbon support SRO can be classified as H4. Both hysteresis indicate the slotted nature of the pores present in materials.

The textural properties of carbon supports are presented in Tables 1 and 2. The starting SRO carbon has a high surface area, a large pore volume and a mesoporous structure. The SRO series supports have a high specific surface area, being in a relatively narrow range 359–435  $m^2/g$ .

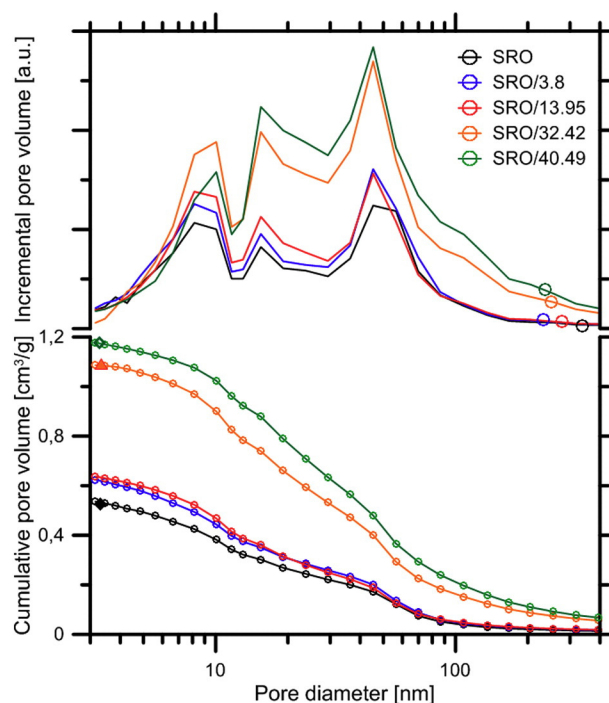


**Fig. 3.** Pore size distributions of carbon supports determined by mercury porosimetry.

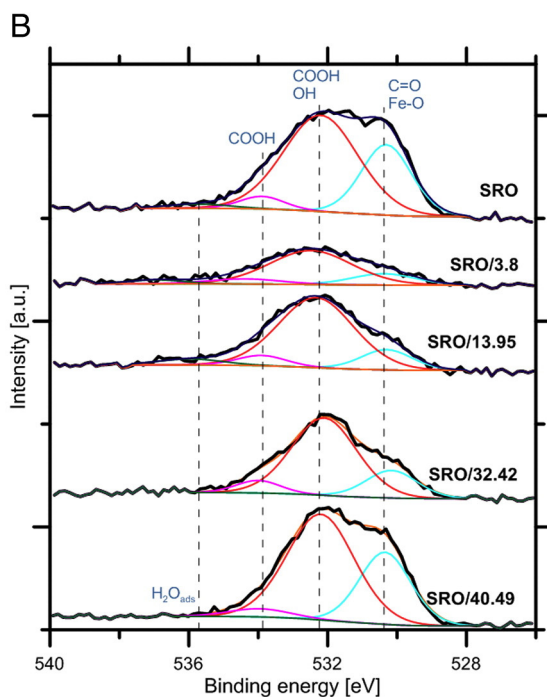
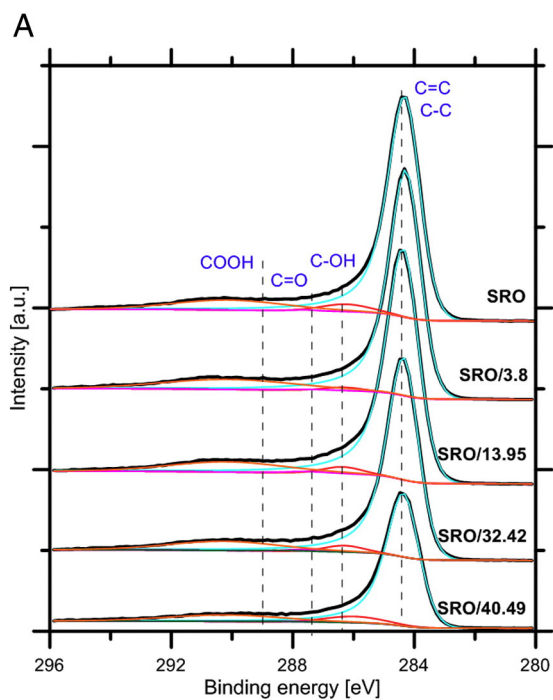


Fig. 4. XPS spectra of the initial carbon (SRO) and modified carbon materials (A – C 1s spectra and B – O 1s spectra).

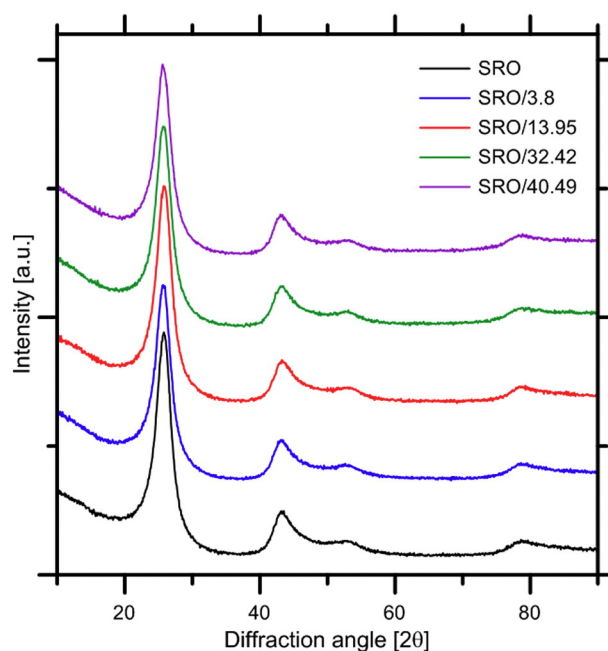


Fig. 5. XRD patterns of the initial carbon SRO and modified carbons.

The SRO, SRO/3.8 and SRO/13.95 samples exhibit similar specific surface areas, with a dominant share of mesopores, and, to a lesser extent, macropores and with a small share of micropores. The total pore volumes of these samples are also similar.

The applied modification of carbon materials at higher levels of gasification (SRO/32.42, SRO/40.49) results in a higher specific surface area and larger pore diameter with a concurrent increase of the pore volume. For these samples a complete disappearance of micropores was observed as a consequence of a large mass loss due to the gasification at steam atmosphere.

Pore size distributions determined by the mercury porosimetry for carbon supports are illustrated in Fig. 3 and parameters of porous structure analysis are given in Table 2.

The pore size distributions of all samples are very similar. Both the starting material SRO and modified supports are characterized by pore distribution with a dominant share of mesopores over the whole range from 2 to 50 nm, i.e. in the range that could be important for the SGS catalyst.

As expected,  $S_{Hg}$  values are similar to those for the  $S_{BET}$  parameter determined by nitrogen physisorption. A series of supports obtained is characterized by high porosity in the range 47–65%. Moreover, with an increasing steam gasification degree, the total porosity and pore volume increase ( $V_c$  and  $V_{mes}$ ). The SRO/3.8, SRO/13.95 samples exhibit rather insignificant increase of  $V_{Hg}$  and  $V_{mHg}$  values, whereas for SRO/32.42 and SRO/40.49 samples over 2-fold increase of  $V_c$  related to the starting material was observed, with a concurrent increase of  $V_{mHg}$ .

Table 3

Surface composition of the carbon supports identified by XPS.

Carbon sample	Oxygen [% at.]					Carbon [% at.]				
	C=O <sup>1</sup>	OH, COOH <sup>2</sup>	COOH <sup>3</sup>	H <sub>2</sub> O <sub>ads</sub> <sup>4</sup>	Total O	C=C, C-C <sup>5</sup>	C-O <sup>6</sup>	C=C <sup>7</sup>	COOH <sup>8</sup>	Total C
SRO	2.1	4.3	0.3	0.2	7.0	87.0	4.0	0.3	0.3	91.5
SRO/3.8	0.5	1.8	0.2	0.1	2.7	95.1	1.6	0.5	0.2	97.3
SRO/13.95	0.6	3.2	0.3	0.2	4.4	92.0	2.9	0.6	0.3	95.6
SRO/32.42	1.0	3.6	0.4	-	5.0	90.5	3.2	1.0	0.4	95.0
SRO/40.49	3.3	6.4	0.5	-	11.0	81.0	6.0	0.7	0.5	87.8

BE [eV]: <sup>1</sup>500.3–500.4, <sup>2</sup>532.1–532.5, <sup>3</sup>533.9–534.4, <sup>4</sup>535.7–536.9, <sup>5</sup>284.3–284.4, <sup>6</sup>286.0–286.4, <sup>7</sup>287.4–287.6, <sup>8</sup>288.4.

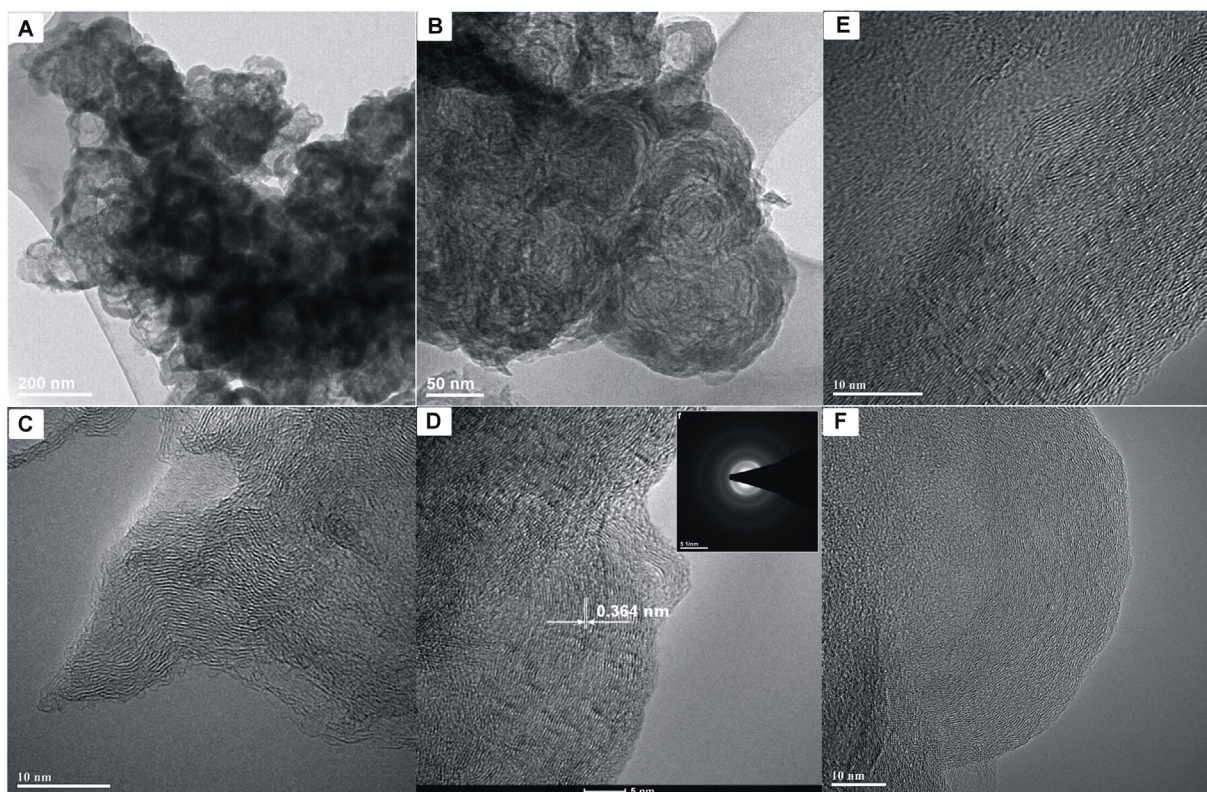


Fig. 6. TEM images of SRO (A–D) and SRO/40.49 (E–F).

### 3.2. Surface composition of the carbon supports

XPS measurements were carried out in order to determine the amount and type of oxygen-containing groups present on the surface of the initial (SRO) and modified carbons. The O 1 s and C 1 s spectra of carbon supports are illustrated in Fig. 4A and B.

Table 3 presents the share of particular carbon and oxygen forms in a series of SRO samples based on the deconvolution of C 1 s and O 1 s spectra (see Fig. 4A and B).

For the SRO samples the highest carbon content corresponds to the C=C and C–C forms and is in the range 87.8–97.3% at. Additionally, in all samples the presence of oxygen-containing functional groups on the carbon surface in an amount from ca. 2.7 to ca. 11.0% at. was observed. In the case of the SRO/3.8 sample, which was subjected to mild steam gasification, more than 2-fold decline of the oxygen-containing functional groups content was noticed in comparison with

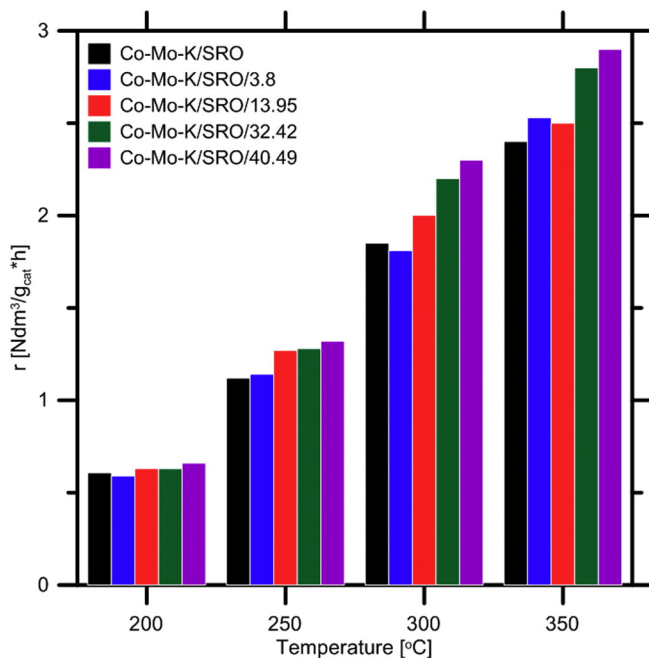


Fig. 7. The comparison of SGS reaction rate of carbon-supported Co–Mo–K catalysts in the range of 200–350 °C.

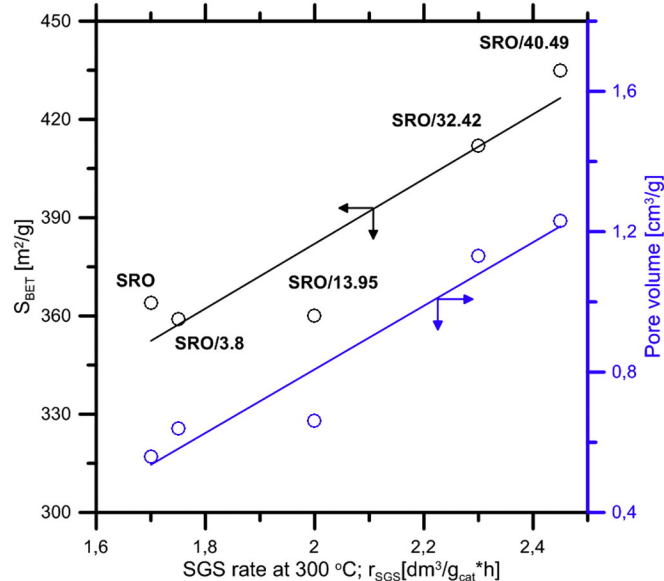


Fig. 8. Correlation between textural parameters of the support and the activity of the catalysts.

the initial SRO sample. This decrease is a side-effect of the treatment at 675 °C. In the case of other samples subjected to deeper gasification, a gradual increase of the content of oxygen-containing functional groups was observed as an effect of the introduction of mainly OH groups as well as of decreasing the carbon content in C=C and C–C forms. The most pronounced influence of the steam gasification process on the content of oxygen-containing functional groups on the carbon support surface was observed for the SRO/40.49 sample, with the highest content corresponding to the C–OH form.

### 3.3. Structure and morphology of the carbon supports

A series of diffraction patterns of the carbon supports is shown in Fig. 5. The XRD pattern of the SRO sample is characterized by a sharp and intensive diffraction line at  $2\theta = 26^\circ$  as well as several lines of lower intensity at diffraction angles  $2\theta$  ranging from  $42.8$  to  $54.0^\circ$  and from  $77.0$  to  $79.0^\circ$ , indicating the presence of partially ordered graphite-like structures already in the starting material. Similar diffraction patterns were obtained for the modified samples (SRO/3.8, SRO/13.95, SRO/32.42, SRO/40.49) – individual diffraction lines show almost identical intensity and shape. Broad lines indicate rather low degree of crystallinity of all samples.

Fig. 6 demonstrates "shell" morphology of high surface area SRO and SRO/40.49 support. The analysis of SRO samples by means of TEM method confirms the results of the XRD measurements concerning the presence in SRO of degenerated or imperfect graphite-like structures. A characteristic feature of those fragments is their partial ordering and the interplanar distance  $d$  similar to that in graphite (0.364 nm vs. 0.335 nm in graphite). Another difference and deviation from the graphite structure is disorientation of the successive graphite-like planes with reference to each other (in graphite these planes are parallel).

The analysis of the SRO/40.49 sample is in accordance with the XRD data, showing a lack of distinct differences in the graphite-like structure (see Fig. 6e and f). The increase of the gasification degree results neither in amorphization processes of the graphite-like structures nor in increasing disorientation of the successive graphite-like planes. Similarly to the SRO sample, the average  $d$  value amounts to 0.365 nm.

### 3.4. SGS activity of carbon-supported Co–Mo–K catalysts

The effect of temperature on the activity in the SGS reaction of the carbon-supported Co–Mo–K catalysts is shown in Fig. 7.

The activity of catalysts under study is quite variable and depends remarkably on a support used. This support effect is more pronounced at higher temperatures, i.e. 300 and 350 °C. The investigated catalysts showed the following order of activity: Co–Mo–K <–Mo–K/SRO/3.8 < Co–Mo–K/SRO/13.95 < Co–Mo–K/SRO/1900/32.42 < Co–Mo–K/SRO/40.49. Among the samples the most active was the catalyst prepared on SRO/40.49.

As the structural features of the supports are quite similar, differences in the catalytic activity should be attributed to the impact of textural properties, i.e. materials are characterized by different specific surface areas, dominant mesopores sizes and mesopores volume.

Correlations between the catalyst activity, surface area of support and pore volume of support are presented in Fig. 8.

The studies of the catalytic properties of Co–Mo–K supported on both NRO [10] and SRO supports in the SGS process confirm the literature data of Lian et al. [9] on Co–Mo–K systems supported on raw active carbon washed only with HNO<sub>3</sub>. The authors emphasize that although potassium addition increases activity substantially it has a negative influence on stability. However the authors concentrated on potassium function but they did not study the influence of the type and texture properties of support.

The modified carbon black supported (SRO-supported) Co–Mo–K catalysts exhibit better catalytic properties in comparison with the

modified active carbon supported ones (NRO-supported) [10]. In contrast to the NRO-based supported catalysts, the activity of SRO-based catalysts cannot be correlated only with the specific surface area.

Other support parameters may influence the activity – in an SRO series, besides the textural parameters mentioned, the materials exhibit a different content of surface functional groups (see Tables 1 and 3).

The impact of oxygen functional groups on the catalytic activity is obvious but no convincing explanation has been proposed so far. It has been known that oxygen functional groups determine the nature of a support [22]. On the other hand, a large number of functional groups on the carbon surface may reduce the catalyst activity by interactions between carbon and molybdenum species, which are similar to Mo–O–Al bonds [2,3]. According to the literature data, functional oxygen-containing groups are probably also formed in the SGS process, due to a high steam content in the process gas [37].

## 4. Conclusions

The effect of steam gasification on the surface composition, textural and structural parameters as well as on the morphology of the carbon supports was investigated. The applied modification of the initial SRO material does not lead to a significant development of the specific surface area but only at higher gasification levels results in a significant increase of the porosity and pore volume. No effect of the steam gasification on structural parameters or morphology of supports was observed. The highest activity in the SGS reaction was measured for the catalyst supported on SRO/40.49. The activity of the catalysts correlates with the textural properties. The high purity and specific surface area as well as advantageous pore distribution (dominant mesopores with a diameter in the range 2–50 nm) – the range that could be important for the usefulness of materials as catalysts supports, it all makes *Sibunit* an attractive material for applications as a support of the industrial low-temperature catalysts for the sour gas shift process.

## References

- [1] M. Inagaki, Pores in carbon materials–importance of their control, *New Carbon Mater.* 24 (2009) 193–232.
- [2] E. Lam, J.H.T. Luong, Carbon materials as catalyst supports and catalysts in the transformation of biomass to fuels and chemicals, *ASC Catal.* 4 (2014) 3393–3410.
- [3] E. Furimsky, *Carbons and Carbon-Supported Catalysts in Hydroprocessing*, RSC, Ottawa, 2009, ISBN 978-0-85404-143-5.
- [4] X.M. Wu, Y.Y. Guo, J.M. Zhou, G.D. Lin, X. Dong, H.B. Zhang, Co-decorated carbon nanotubes as a promoter of Co–Mo–K oxide catalyst for synthesis of higher alcohols from syngas, *Appl. Catal. A* 340 (2008) 87–97.
- [5] S. Zaman, S. KJ, A review of molybdenum catalysts for synthesis gas conversion to alcohols: catalysts, mechanisms and kinetics, *Catal. Rev. Sci. Eng.* 54 (2012) 41–132.
- [6] M. Lv, W. Xie, S. Sun, G. Wu, L. Zheng, S. Chu, C. Gao, J. Bao, Activated-carbon-supported K–Co–Mo catalysts for synthesis of higher alcohols from syngas, *Catal. Sci. Technol.* 5 (2015) 2925–2934.
- [7] M. Bonarowska, J. Pielaszek, V.A. Semikolenov, Z. Karpiński, Pd–Au/sibunit carbon catalysts: characterization and catalytic activity in hydrodechlorination of dichlorodifluoromethane (CFC-12), *J. Catal.* 209 (2002) 528–538.
- [8] T. Zhengli, X. Huining, Z. Runduo, Z. ZiSheng, S. Kaliaguine, Potential to use mesoporous carbon as catalyst support for hydrodesulfurization, *New Carbon Mater.* 24 (4) (2009) 333–343.
- [9] Y. Lian, R.F. Xiao, W. Fang, Y. Yang, Potassium-decorated active carbon supported Co–Mo based catalyst for water-gas shift reaction, *J. Nat. Gas Chem.* 20 (2011) 77–83.
- [10] K. Antoniak-Jurak, P. Kowalik, W. Próchniak, W. Raróg-Pilecka, P. Kuśtrowski, J. Ryczkowski, Sour gas shift process over sulfided Co–Mo–K catalysts supported on carbon material – support characterization and catalytic activity, *Fuel Process. Technol.* 138 (2015) 305–313.
- [11] P. Smirniotis, K. Gunugunuri, *Research Developments and Applications, Chapter 4 - WGS Reaction over Co–Mo Sulfided Catalysts* (2015) 101–126 ISBN: 9780124201545.
- [12] S.S. Hla, G.J. Duffy, L.D. Morpeth, A. Cousins, D.G. Roberts, J.H. Edwards, Investigation into the performance of a Co–Mo based sour shift catalyst using simulated coal derived syngases, *Int. J. Hydrog. Energy* 36 (2011) 6638–6645.
- [13] S.S. Hla, G.J. Duffy, L.D. Morpeth, A. Cousins, D.G. Roberts, J.H. Edwards, D. Park, Catalysts for water-gas shift processing of coal-derived syngases, *Asia Pac. J. Chem. Eng.* 5 (2010) 585–592.
- [14] A.R. de la Osa, A. de Lucas, J.L. Valverde, A. Romero, I. Monteagudo, P. Sanchez, Performance of a sulfur-resistant commercial WGS catalyst employing industrial coal-derived syngas feed, *Int. J. Hydrog. Energy* 36 (2011) 1–12.

- [15] B. Liu, Q. Zong, P.P. Edwards, F. Zou, X. Du, Z. Jiang, T. Xiao, H. AlMegren, Effect of titania addition on the performance of CoMo/Al<sub>2</sub>O<sub>3</sub> sour water gas shift catalysts under lean steam to gas ratio conditions, *Ind. Eng. Chem. Res.* 51 (2012) 11674–11680.
- [16] B. Liu, Q. Zong, X. Du, Z. Zhang, T. Xiao, H. AlMegren, Novel sour water gas shift catalyst (SWGS) for lean steam to gas ratio applications, *Fuel Process. Technol.* 134 (2015) 65–72.
- [17] A.R. de la Osa, A. De Lucas, A. Romero, P. Casero, J.L. Valverde, P. Sánchez, High pressure water gas shift performance over a commercial non-sulfide CoMo catalyst using industrial coal-derived syngas, *Fuel* 97 (2012) 428–434.
- [18] K. Antoniak, P. Kowalik, W. Próchniak, M. Konkol, A. Wach, P. Kuśtrowski, J. Ryczkowski, Effect of flash calcined alumina support and potassium doping on the activity, *Appl. Catal. A* 423–424 (2012) 114–120.
- [19] K. Antoniak-Jurak, P. Kowalik, W. Próchniak, Active alumina prepared by flash calcination as a support of Co–Mo–K catalysts for sour gas shift process, *Przem Chem.* 93 (2014) 1141–1145.
- [20] D. Nikolova, R. Edreva-Kardjieva, E.M. Serwicka, R. Dula, T. Grozeva, State of the components of (K)(Ni)W/Al<sub>2</sub>O<sub>3</sub> catalysts as oxide precursors and after water-gas shift reaction in the presence of Sulphur, *Appl. Catal. A* 480 (2014) 108–119.
- [21] T. Sasaki, T. Suzuki, Sulfide molybdenum catalysts for water–gas shift reaction: influence of the kind of promoters and supports to generate MoS<sub>2</sub>, *Appl. Catal. A* 484 (2014) 79–83.
- [22] M. Laniecki, M. Małecka-Gryc, F. Domka, Water–gas shift reaction over sulfide molybdenum catalysts: I. Alumina, titania and zirconia-supported catalysts, *Appl. Catal. A* 196 (2000) 293–303.
- [23] M. Laniecki, M. Ignacik, Water–gas shift reaction over sulfided molybdenum catalysts supported on TiO<sub>2</sub>–ZrO<sub>2</sub> mixed oxides. Support characterization and catalytic activity, *Catal. Today* 116 (2006) 400–407.
- [24] K. Antoniak, Alumina and carbon supported Co–Mo catalysts promoted with alkali for Sour Gas Shift Reaction (PhD Dissertation) UMCS, Lublin, 2013.
- [25] Y. Zhang, G. Zhang, Y. Zhao, X. Li, Y. Sun, Y. Xu, Ce–K–promoted Co–Mo/Al<sub>2</sub>O<sub>3</sub> catalysts for the water gas shift reaction, *Int. J. Hydrog. Energy* 37 (2012) 6363–6371.
- [26] T.M. Roberge, S.O. Blavo, C. Holt, P.H. Matter, J.H. Kuhn, Effect of molybdenum on the sulfur-tolerance of cerium–cobalt mixed oxide water–gas shift catalysts, *Top. Catal.* 56 (2013) 1892–1898.
- [27] F. RR, The role of carbon materials in heterogeneous catalysis, *Carbon* 36 (1998) 159–175.
- [28] H. Wang, Z. Li, E. Wang, C. Lin, Y. Shang, G. Ding, X. Ma, S. Qin, Q. Sun, Effect of composite supports on the methanation activity of Co–Mo-based Sulphur-resistant catalysts, *J. Nat. Gas Chem.* 21 (2012) 767–773.
- [29] S. Suppan, J. Trawczyński, J. Kaczmarczyk, G. Djega-Mariadassou, A. Hynaux, C. Sayag, Effect of carbon black composite (CBC) support properties on hydrodesulfurization performance of sulfided Mo and Co, and carburized Mo, catalysts, *Appl. Catal. A Gen.* 280 (2005) 209–214.
- [30] P. Gheek, S. Suppan, J. Trawczyński, A. Hynaux, C. Sayag, G. Djega-Mariadassou, Carbon black composites-supports of HDS catalyst, *Catal. Today* 119 (2007) 19–22.
- [31] V.B. Felonov, V.A. Likhobobov, A.Y. Derevyankin, M.S. Mel'gunov, Porous carbon materials prepared from C1 ± C3 hydrocarbons, *Catal. Today* 42 (1998) 341–345.
- [32] V. Rao, P.A. Simonov, E.R. Savinova, G.V. Plaksin, S.V. Cherepanova, G.N. Kryukova, U. Stimming, The influence of carbon support porosity on the activity of PtRu/sibunit anode catalysts for methanol oxidation, *J. Power Sources* 145 (2005) 178–187.
- [33] H. Topsøe, The role of Co–Mo–S type structures in hydrotreating catalysts, *Appl. Catal. A* 322 (2007) 3–8.
- [34] A.K. Tuxen, H.G. Führtbauer, B. Temel, B. Hinnemann, H. Topsøe, K.G. Knudsen, F. Besenbacher, J.V. Lauritsen, Atomic-scale insight into adsorption of sterically hindered dibenzothiophenes on MoS<sub>2</sub> and Co–Mo–S hydrotreating catalysts, *J. Catal.* 295 (2012) 146–154.
- [35] A.I. Dugulan, E.J.M. Hensen, J.A.R. van Veen, High-pressure sulfidation of a calcined Co Mo/Al<sub>2</sub>O<sub>3</sub> hydrodesulfurization catalyst, *Catal. Today* 130 (2008) 126–134.
- [36] F. Rouquerol, J. Rouquerol, K. Sing, Adsorption by Powders and Porous Solids, Principle, Methodology and Applications, Academic Press, New York, 1999.
- [37] A.A. Andreev, V.J. Kafedjyjsky, R.M. Edreva-Kardjieva, Active forms for water–gas shift reaction on NiMo-sulfide catalysts, *Appl. Catal. A* 179 (1999) 223–228.